JOURNAL OF CATALYSIS 73, 377–386 (1982)

Fouling of a Platinum Reforming Catalyst Accompanying the Dehydrogenation of Methyl Cyclohexane

L. W. JOSSENS AND E. E. PETERSEN

Chemical Engineering Department, University of California, Berkeley, California 94720

Received April 16, 1981; revised October 5, 1981

Fouling of a platinum reforming catalyst during the dehydrogenation of methylcyclohexane was studied under reaction conditions varying between 350 and 400°C, 200 and 600 Torr hydrogen, 10 and 30 Torr MCH, and 2 and 12 Torr toluene. Each experiment was carried out at constant temperature and constant reaction mixture composition. During the early stages, the deactivation was totally reversible, that is, the initial activity of the catalyst was recoverable in a stream of hydrogen. The deactivation during this stage was essentially zero order and the activation energy of the deactivation rate was 8 Kcal/gmole. At times in excess of about 40 min on stream, the deactivation was only partially reversible and the rate of deactivation was proportional to the rate of dehydrogenation of MCH. The activation energy of the deactivation rate in the latter stage was 39 Kcal/gmole.

INTRODUCTION

Understanding the deactivation characteristics of a naptha reforming catalyst is important not only in the operation of a commercial reforming unit, but also in the future development of more stable catalysts. Catalyst deactivation can occur through several routes the most common of which are fouling, impurity poisoning, and sintering.

The fouling characteristics of catalysts using model reforming reactions can be followed in laboratory test reactors in which very severe conditions are maintained to accelerate the deactivation process. This paper concerns the accelerated fouling behavior of a chlorinated Pt-γ-alumina catalyst using the dehydrogenation of methylcyclohexane (MCH) as a model reforming reaction. This highly selective dehydrogenation reaction yields toluene as its major product, and should serve as a probe to determine the effect of fouling on the metallic sites of this bifunctional reforming catalyst (*1*).

Constant reactant and product concentrations were maintained in each of the fouling studies presented in this paper. This experimental approach allows the direct comparison of observed reaction rates for a deactivated catalyst to the initial reaction rate. In addition, the time response of the system is rapid thereby obviating the need for long extrapolations of rate data back to zero time in order to obtain an initial reaction rate.

In an adjoining paper, changes in the fouling characteristics resulting from the addition of rhenium to the platinum reforming catalyst and by the effects of presulfiding each of the catalysts will be presented.

EXPERIMENTAL

Apparatus. Two reactors are used in this study: an external recycle single-pellet reactor and an external recycle differential reactor. Details of the apparatus, pretreatment conditions, reaction mixture, and catalyst were described previously (*2*).

RESULTS AND DISCUSSION

Initial rate kinetics. The kinetic behavior of this catalyst in the non-deactivated state is important for two reasons: first, it facilitates the comparison of reaction rates determined for a deactivated catalyst at

0021-9517/82/020377-10$02.00/0

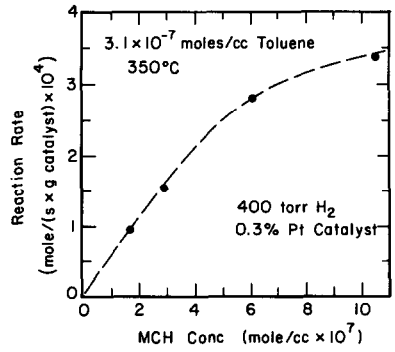

FIG. 1. MCH initial rate kinetics.

specified temperature and reaction mixture composition to that of a fresh catalyst at identical conditions, and second, it serves as a reference to determine if there are mechanistic changes in the model reaction as the catalyst deactivates. The ability to determine initial reaction rate kinetics at reaction conditions that will yield catalyst fouling depends upon the low nominal residence time of the reactor system and the completely reversible behavior of the short-term deactivation reaction.

Figure 1 shows the production rate of toluene resulting from the dehydrogenation of MCH at 350°C and 400 Torr hydrogen pressure. Selectivity for the production of toluene is in excess of 95% at these reaction conditions. The measured MCH dehydrogenation rates shown in Fig. 1 are not masked by the reverse reaction of toluene hydrogenation because the equilibrium strongly favors the forward reaction (thermodynamic data from Ref. (*3*)).

The dehydrogenation reaction appears to be first order in MCH concentration below 6×10^{-7} gmole/cm^3, whereas at higher concentrations the order decreases and may approach zero order asymptotically. This zero-order dependency would be in agreement with that reported by Sinfelt *et al.* (*4*) who used MCH concentrations in excess of 15×10^{-7} gmole/cm^3 while the first-order behavior is consistent with the results reported by Herz *et al.* (*1*) for the dehydrogenation of cyclohexane at low concentrations over a platinum single-crystal catalyst.

Under the reaction conditions of 350°C and 400 Torr hydrogen pressure, product inhibition is observed. The effect can be expressed empirically as toluene concentration to the negative 0.33 power as shown in Fig. 2. Increasing temperature increases toluene inhibition while increasing hydrogen partial pressure strongly decreases toluene inhibition. For example, at 425°C and 1 atm hydrogen partial pressure, there is virtually no toluene inhibition. This is in agreement with the work of Sinfelt *et al.* (*4*) whose results were measured at hydrogen partial pressures of 1 atm or more and a temperature of 315°C. In related studies, product inhibition has been reported in three studies involving the dehydrogenation of cyclohexane: by Mencier *et al.* (*5*) using a Pt–SiO_2 catalyst, by Andreev *et al.* (*6*) using a Ni–ZnO catalyst, and by Herz *et al.* (*1*) using a platinum single-crystal catalyst. All three studies were carried out at hydrogen partial pressures of less than 1 atm. Herz *et al.* (*1*) also found marked reduction in inhibition with increasing hydrogen partial pressure.

The effect of varying hydrogen partial pressure on initial reaction rates is complicated by the fact that the reaction order with respect to toluene concentration is a function of the hydrogen partial pressure. Between 600 and 1000 Torr a zero order behavior is observed with respect to hydrogen partial pressures. Below 600 Torr hy-

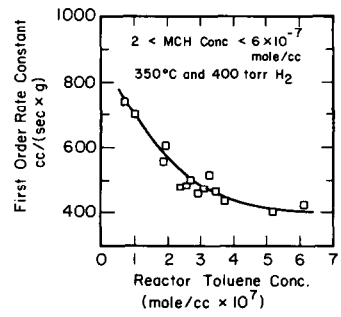

FIG. 2. Toluene inhibition.

drogen partial pressure the initial reaction rates increase with increasing hydrogen partial pressure. For example, the ratio of two initial rates, one conducted at 600 Torr and the other at 200 Torr, is 1.4. Product inhibition effects are not presented at 200 Torr because rapid self-deactivation occurs under these conditions as shown in Fig. 6.

An Arrhenius plot for toluene product is shown in Fig. 3. The apparent energy of activation is about 17 Kcal/mole for temperature between 200 and 350°C. At temperatures in excess of 370°C, the apparent activation energy decreases owing to increased toluene inhibition. Over the temperature range of this plot, the effectiveness factor changes less than 10%.

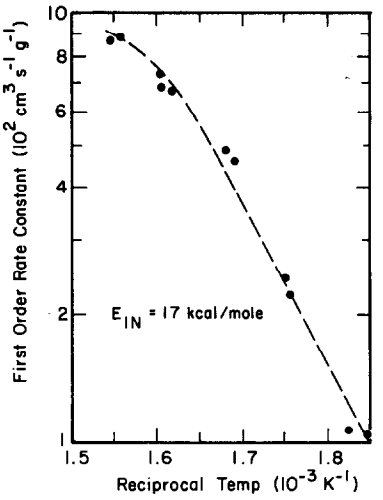

FIG. 3. Arrhenius plot of initial MCH reaction rates.

The reaction rates presented above are very much larger than those presented in the literature for methylcyclohexane (*4*, *7*).

There are many reasons why the experimentally determined reaction rates can be low, such as intraparticle mass transfer limitations and fouling of the catalyst prior to the initial reaction rate determination. From a study to determine intraparticle mass transfer limitations it is known that a catalytic effectiveness factor of 0.4 would be obtained by just increasing the size of the catalyst particles to 0.05 cm, while the half-life of this catalyst during the dehydrogenation of MCH is approximately 7 min at 352°C and 400 Torr hydrogen partial pressure.

Fouling rate kinetics. There are four system variables that determine the fouling characteristics of a Pt catalyst accompanying the dehydrogenation of MCH. They are: MCH concentration, toluene concentration, hydrogen partial pressure, and cat-

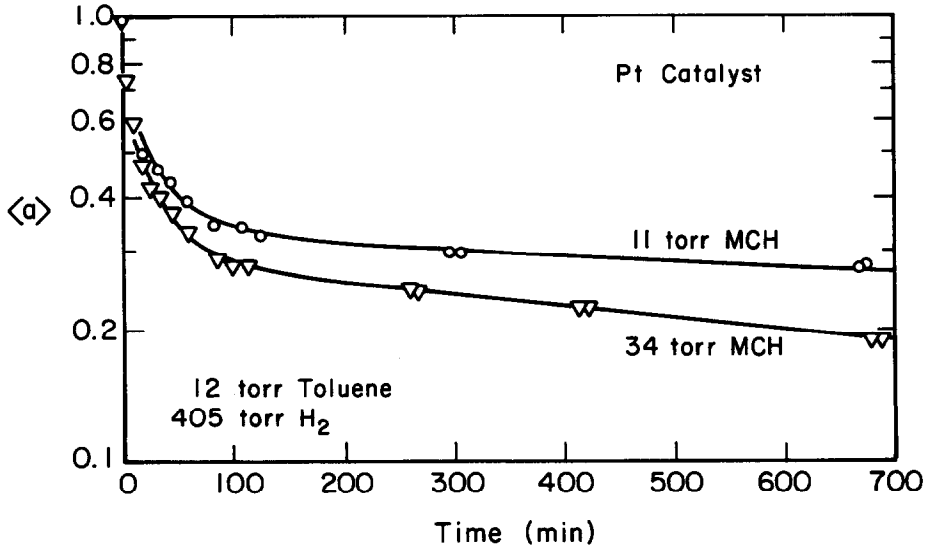

FIG. 4. MCH deactivation kinetics at constant reactant concentration at 352°C.

alyst temperature. Figures 4 through 7 are characteristic plots that demonstrate the effect of each system variable. In each of these plots, three variables are held approximately constant to demonstrate the effect of the fourth. Deactivation data are expressed as catalytic dehydrogenation activity versus time. Catalytic activity, $\langle a \rangle$, at time t is defined as the ratio of observed reaction rate at a specified time, $R(t)$, to initial reaction rate, R_0, determined 15 sec after the initiation of the deactivation experiment.

Each deactivation curve has a similar characteristic shape: a rapid deactivation for about the first 40 min, designated as Region I, followed by a much slower deactivation, designated as Region II. Figures 4 and 5 respectively, present the effect of MCH concentration and toluene concentration on the self-deactivation behavior of the Pt catalyst. During approximately the first 20 min there appear to be only small differences in behavior with varying MCH or toluene concentration. In Region II, the logarithm of activity, ln $\langle a \rangle$, varies approximately as a linear function of time. This characteristic linear behavior is also displayed in Figs. 6 and 7, respectively. The linear relationship between ln $\langle a \rangle$ and time in Region II leads to the following proportionality

$$\frac{d[\ln\langle a \rangle]}{dt} = -k^*. \tag{1}$$

Although the empirically determined values of k^* differ from one fouling experiment to another they can all be related by a simple proportionality to initial reaction rate

$$k^* = kR_0, \tag{2}$$

where k is a simple constant for all experiments at a given temperature and hydrogen partial pressure. Thus in Fig. 4, positive-order MCH kinetics results in an increased initial reaction rate for the higher MCH concentration case and the observed deactivation rate is higher. Similarly, in Fig. 5, decreasing the toluene product concentration increases the initial reaction and deactivation rates. Therefore, Eq. (1) can be written as

$$\frac{d[\ln\langle a \rangle]}{dt} = -kR_0, \tag{3}$$

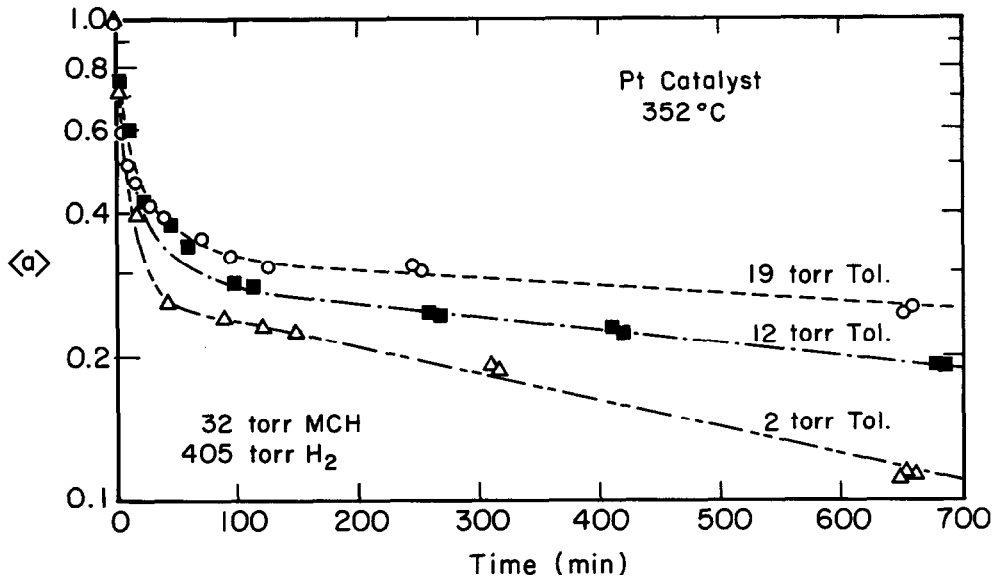

FIG. 5. Toluene deactivation kinetics at constant reactant concentration.

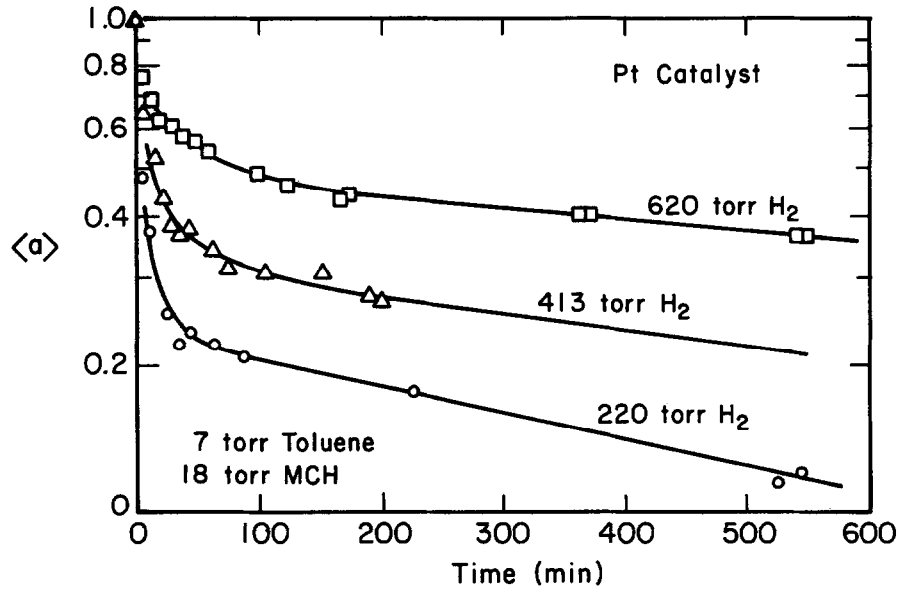

FIG. 6. Hydrogen deactivation kinetics at constant reactant concentration at 352°C.

Figure 8 shows this relationship as determined at a equal to 0.25.

Integration of Eq. (3) leads to

$$\langle a \rangle = \langle a_{INT} \rangle \exp(-kR_0 t), \quad (4)$$

where $\langle a_{INT} \rangle$ is a pseudoinitial activity generated by extrapolating the long-term deactivation curve back to zero time, or

$$R(t) = \langle a_{INT} \rangle R_0 \exp(-kR_0 t). \quad (5)$$

Equation (5) implicitly accounts for the effect of toluene concentration on the fouling

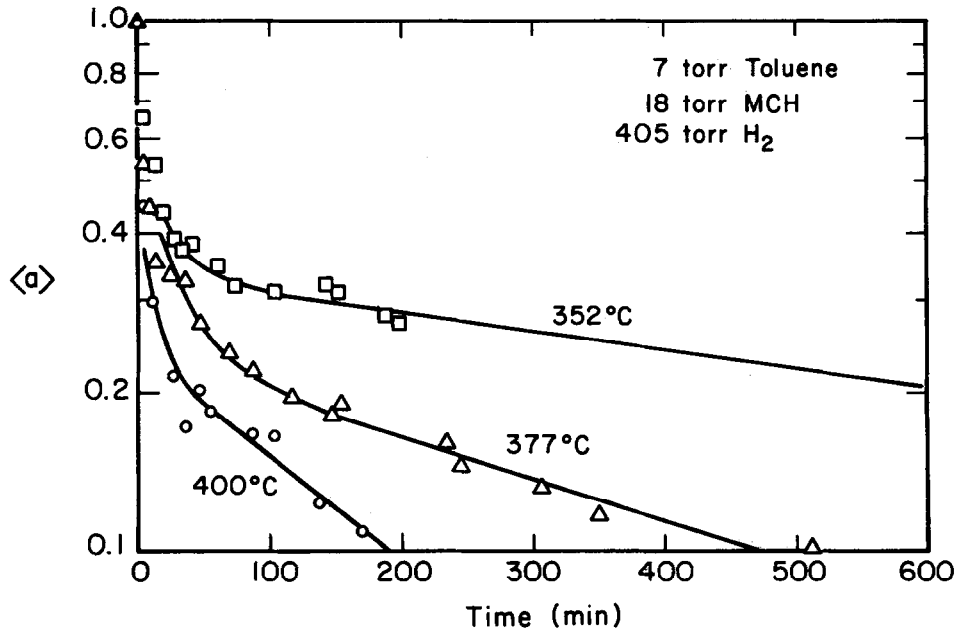

FIG. 7. Thermal characteristics of a Pt catalyst, constant reactant concentration.

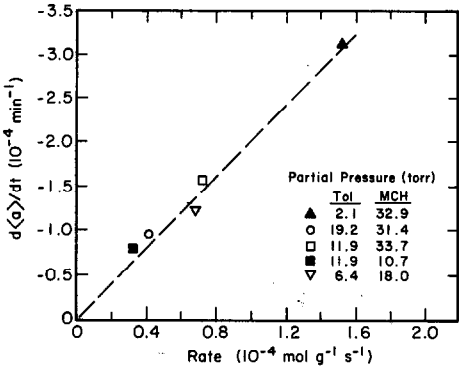

FIG. 8. Time rate of change of activity for a Pt catalyst evaluated at $\langle a \rangle = 0.25$.

rate during the long-term deactivation period by altering the value of R_0. This equation predicts a decreased rate of deactivation for increased toluene concentrations. The work of Myers *et al.* (*8*) is consistent with this idea. Myers found that by switching from a naptha–hydrogen feed to a toluene–hydrogen feed and then back again to a naptha–hydrogen feed he could increase the yield from a partially deactivated platinum reforming catalyst. Tetenyi and Babernics (*9*) in their work on chemisorption of carbon-labeled benzene on platinum found that chemisorbed benzene is reversible in a stream of flowing hydrogen. This indicates that the benzene ring alone does not polymerize to form coke.

Another distinguishing characteristic between the observed deactivation behavior of Regions I and II is that short-term deactivation is totally reversible. Removing reactants from the inlet feed stream while maintaining constant hydrogen partial pressure will result in increased activity for a partially deactivated catalyst. This partial reversibility was noted by early workers on Pt-γ reforming catalysts (*8*). If MCH is removed from the inlet feed stream at a time such that the catalytic activity is still greater than $\langle a_{INT} \rangle$, the lost activity is totally reversible by a flowing stream of hydrogen at the temperature and hydrogen partial pressure of the deactivation experiment. Allowing the deactivation to continue beyond an activity level equal to $\langle a_{INT} \rangle$ results in a catalyst which cannot be totally regenerated in hydrogen at reaction operating conditions in a time span of about 8 hr. Activity of this partially regenerated catalyst $\langle a_{REG} \rangle$ was found to be approximately related to the deactivated state of the catalyst at the time MCH is removed from the feed stream, $\langle a \rangle$, by

$$\frac{\langle a_{REG} \rangle}{\langle a \rangle} = \frac{1}{\langle a_{INT} \rangle}. \tag{6}$$

Values for $\langle a_{INT} \rangle$ are only weakly dependent on initial reaction rate, as shown in Figs. 4 and 5, and temperature, Fig. 7. As shown in Fig. 6, the hydrogen partial pressure has the greatest effect on the magnitude of $\langle a_{INT} \rangle$. The total reversible nature of the self-deactivation in Region I and Eq. (6) suggest that $\langle a_{INT} \rangle$ can be correlated to hydrogen partial pressure by an equilibrium expression of the form

$$K = \frac{(1 - \langle a_{INT} \rangle)}{\langle a_{INT} \rangle} [H_2], \tag{7}$$

where $\langle a_{INT} \rangle$ is proportional to the active surface and $(1 - \langle a_{INT} \rangle)$ is proportional to the reversibly poisoned surface. The nominal linear behavior of Fig. 9 suggests the plausibility of an equilibrium between active and reversibly poisoned sites in Region I.

Increased hydrogen partial pressures reduces the deactivation rate during Region II. This effect, though monotonic with hydrogen partial pressures, does not correlate as well as the effect of $\langle a_{INT} \rangle$ versus hydrogen partial pressure. A possible explanation for the observed relationship between long-term deactivation rates and hydrogen pressure is that both active and reversibly poisoned sites interact with a reaction intermediate to yield an irreversibly poisoned site. This can be stated as

$$\frac{d\langle a_{IRR} \rangle}{dt} = k_1 \langle a \rangle R_0 + k_2 \langle a_{REV} \rangle R_0, \tag{8}$$

where $\langle a_{IRR} \rangle$ is the fraction of the surface irreversibly poisoned and $\langle a_{REV} \rangle$ is the frac-

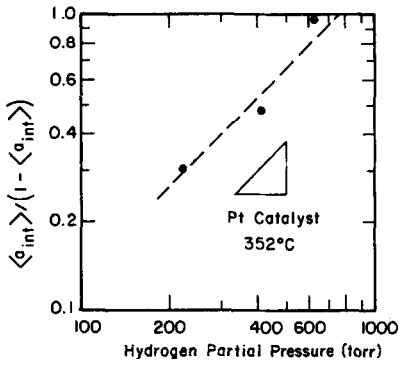

FIG. 9. Transition activity.

tion of the surface reversibly poisoned. By use of Eqs. (6) and (7) and a site balance

$$\langle a_{IRR}\rangle + \langle a_{REV}\rangle + \langle a\rangle = 1, \quad (9)$$

Eq. (8) can be written as

$$\frac{d\langle a\rangle}{dt} = -\langle a\rangle R_0 \left\{\frac{k_1[H_2] + k_2K}{[H_2] + K}\right\}, \quad (10)$$

where the k of Eq. (3) is now

$$k = \frac{k_1[H_2] + k_2K}{[H_2] + K}. \quad (11)$$

Equation 11 displays a nonlinear relationship between k and hydrogen pressure.

It also follows quite generally from Eqs. (6), (7), and (9) that

$$\langle a_{IRR}\rangle = 1 - \left[1 + \frac{K}{[H_2]}\right]\langle a\rangle \quad (12)$$

and

$$\frac{d\langle a_{IRR}\rangle}{dt} = -\left[1 + \frac{K}{[H_2]}\right]\frac{d\langle a\rangle}{dt}. \quad (13)$$

From these expressions it is evident that at elevated hydrogen pressures the amount of reversible poisoning is reduced and in the limit the change in activity during the long-term deactivation period is due to irreversible poisoning.

As already noted in Figs. 4 through 7 there are differences between the observed deactivation characteristics of Regions I and II. Temperature effects in these regions are also quite different. The following three activation energies describe the effect of temperature on observed deactivation behavior:

(1) E_{IN}, energy of activation for initial rates at a fixed toluene concentration,

$$R_0 = A_1(C_{MCH}) \exp\left(-\frac{E_{IN}}{RT}\right). \quad (14)$$

(2) E_{SD}, energy of activation for deactivation at time zero, Fig. 10,

$$\frac{d\langle a\rangle}{dt} = A_2 \exp\left(-\frac{E_{SD}}{RT}\right). \quad (15)$$

(3) E_{LD}, energy of activation for the slow deactivation period, Fig. 11, deactivation rates determined at $\langle a\rangle = 0.25$,

$$\frac{d[\ln\langle a\rangle]}{dt} = R_0A_3 \exp\left(-\frac{E_{LD}}{RT}\right). \quad (16)$$

In determining the energy of activation for deactivation at time zero (E_{SD}) it is necessary to approximate the derivative, i.e.,

$$\frac{d\langle a\rangle}{dt} \approx \frac{\Delta\langle a\rangle}{\Delta t}, \quad (17)$$

where Δt is taken between $t = 0.25$ and $t = 6$ min and $\Delta\langle a\rangle$ is calculated from the corresponding activities.

Numerical values for these activation energies are:

(1) 17 Kcal/mole for initial rate,

(2) 8 Kcal/mole for the rapid deactivation period, Region I.

(3) 39 Kcal/mole for the slow deactivation period, Region II.

As shown by the magnitude of these en-

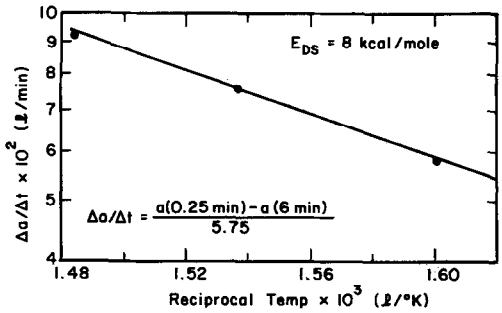

FIG. 10. Arrhenius plot for the rate of initial deactivation of a Pt Catalyst, evaluated at 405 Torr H_2.

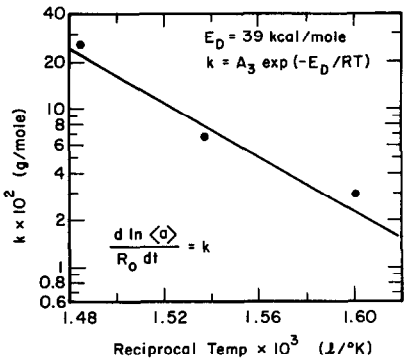

FIG. 11. Arrhenius plot for the long-term deactivation of a Pt catalyst, evaluated at $\langle a \rangle = 0.25$ and 405 Torr H_2.

ergies of activation, temperature is a complex variable, and there appears to be at least two district deactivation domains. The deactivation during Region I is rapid and reversible while that in Region II is slow and partially reversible. Deactivation in Region I is not strongly dependent on temperature and only slightly dependent on reactant and product concentrations. Slow deactivation is strongly dependent on temperature and intrinsic initial reaction rate.

Additional information concerning the reversible deactivation behavior of Region I can be derived from a single-pellet experiment. The philosophy behind the use of the single-pellet experiment is that it permits the experimental measurement of the reactant concentration at the center of a pellet. This technique has been described in detail elsewhere (*10*). Briefly, catalytic particles are pressed into a slab configuration of which only one surface of this slab is exposed to bulk reactant flow. The other surface then becomes equilvalent to the center-plane of a pellet which is twice as thick and has both surfaces exposed to bulk reactant flow. The reactant concentration at the simulated center-plane is followed as a function of time along with the bulk reactant concentration during a deactivation experiment. A plot of apparent catalytic activity versus center-plane concentration permits discrimination among possible deactivation models. Reduced center-plane concentration is defined as

$$\frac{\Psi(t) - \Psi(0)}{1 - \Psi(0)},$$

where $\Psi(t)$ is equal to the ratio of the center-plane reactant concentration to the bulk reactant concentration at time t.

The single-pellet results for the dehydrogenation of MCH are presented in Fig. 12 for two pellets each having a thickness of 0.1 cm and an initial catalytic effectiveness factor 0.21. In addition to the experimental results, three limiting deactivation cases are also presented on this plot: pore mouth poisoning which is indicative of either reactant fouling or strong impurity poisoning, uniform poisoning which indicates that reactant and products are equally effective in fouling, and core poisoning which is indicative of product fouling. These curves are generated for the dehydrogenation of MCH using slab geometry and physical parameters which match the experimental pellets. The dehydrogenation is described by first-order kinetics in MCH and negative 0.33 order kinetics in toluene.

Data taken during the reversible deactivation period, Region I, have apparent catalytic activities between 1.0 and 0.6. The data for this period suggest that the deactivation is caused by both MCH and toluene and with the toluene being slightly more effective as a deactivating agent.

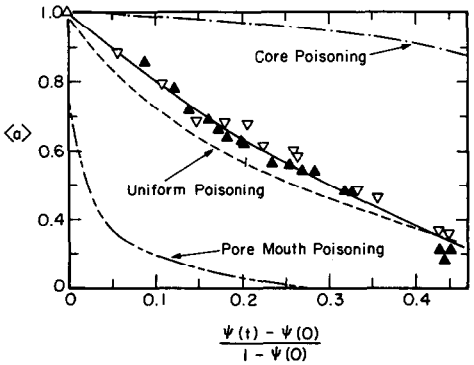

FIG. 12. Diagnostic deactivation curves evaluated at 405 Torr hydrogen and 352°C.

From experiments conducted with the differential recycle reactor the extent of deactivation occurring in the initial deactivation period was found to be defined by $\langle a_{INT} \rangle$, whose magnitude is relatively independent of the hydrocarbon concentrations. Thus, data from both reactors suggest that the deactivation in the initial period is nearly zero order in MCH and toluene concentration.

DEACTIVATION MODEL

A phenomenological model capable of describing the fouling of a platinum reforming catalyst during the dehydrogenation of MCH must be compatible with the following observed deactivation behavior:

A. During the initial deactivation period:

(1) The deactivation kinetics are nearly zero order in MCH and toluene concentration.

(2) The extent of initial deactivation as measured by $\langle a_{INT} \rangle$ is correlated by a simple equilibrium expression involving hydrogen.

(3) Deactivation is totally reversible in a stream of flowing hydrogen at the experimental conditions.

(4) The energy of activation is low.

B. During long-term deactivation:

(1) The rate of deactivation is proportional to overall MCH dehydrogenation rate.

(2) Deactivation is partially reversible in a stream of flowing hydrogen at experimental conditions.

(3) The energy of activation is large.

These characteristics suggest at least a two-step poisoning model. We postulate that during the short-term deactivation period the metallic surface develops an equilibrium state between active and reversible nonactive sites. This equilibrium is established through a simple dehydrogenation step with the resultant product being a reversible nonactive species on the catalyst surface.

The long-term deactivation is attributed to the subsequent reaction between an intermediate generated from the overall MCH dehydrogenation reaction with some surface species. This final reaction produces an irreversible deactivated site.

The observed structure insensitivity of the MCH dehydrogenation reaction and the agreement between the MCH dehydrogenation kinetics for fresh and spent catalyst suggest that the MCH dehydrogenation mechanism remains constant during a deactivation experiment. This evidence suggests further that the surface concentration of reaction intermediates involved in the production of irreversible deactivated sites should remain constant through a deactivation experiment. Analytically this would result in an expression for the time rate of change of catalytic activity which would be proportional to the initial reaction rate times the catalytic activity.

The dehydrogenation of MCH is thought to occur either on a clean platinum surface or on a carbonaceous overlayer covering the metallic platinum surface (*1*). Delineation of the true active surface is not conclusively possible from the characteristics observed by these authors. But, the assertion that the active surface is a carbonaceous overlayer seems to best fit the observed deactivation characteristics. In their work on the dehydrogenation of cyclohexane over a platinum single crystal, Davis and Somorjai (*11*) found that a complete carbonaceous overlayer developed during the first 10 to 200 sec of contact at a reaction temperature of 150°C and hydrogenation concentration of 10^{-6} Torr. They also observed that the overlayer coverage increased with reaction temperature, was effectively irreversible at temperatures in excess of 120°C and was not a function of hydrocarbon concentration. The very fast development of a carbonaceous overlayer followed by the equilibration of this overlayer into active and reversibly poisoned sites is a possible explanation for the near zero-order dependency of initial deactivation rates to hydrocarbon concentrations found in this work.

ACKNOWLEDGMENTS

This work was supported in part by funds from the National Science Foundation, Grant ENG. 79-10412. The catalyst was generously supplied to us by Chevron Research Corporation.

REFERENCES

1. Herz, R. K., Gillespie, W. D., Petersen, E. E., and Sormorjai, G. A., *J. Catal.* **67,** 371 (1981).
2. Jossens, L. W., and Petersen, E. E., *J. Catal.*, **73,** 366 (1982).
3. "Selected Values of Physical and Thermodynamic Properties of Hydrocarbons and Related Compounds," A. P. I. Research Project #44. Carnegie Press, Inc., New York, 1953.
4. Sinfelt, J. H., Hurwitz, H., and Shulman, R. A., *J. Phys. Chem.* **64,** 1559 (1560).
5. Mencier, B., Figueras, F., de Mourques, L., and Trambouze, Y., *J. Chim. Phys.* **66,** 171 (1969).
6. Andreev, A. A., Shopov, D. M., and Kiperman, S. L., *Kinet. Katal.* **7**(6), 1092 (1966).
7. Wolf, E. E., and Petersen, E. E., *J. Catal.* **46,** 190 (1970).
8. Myers, C. G., Long, W. H., and Weisz, P. B., *Ind. Eng. Chem.* **53**(4), 299 (1961).
9. Tetenyi, P., and Babernics, L., *J. Catal.* **8,** 215 (1967).
10. Petersen, E. E., *Exp. Methods Catal. Res.* **2,** 7 (1976).
11. Davis, S. M., and Somorjai, G. A., *J. Catal.* **65,** 78 (1980).